Fermion-number susceptibility in lattice gauge theory

Steven Gottlieb
Department of Physics, Indiana University, Bloomington, Indiana 47405

W. Liu
Department of Physics, University of California, La Jolla, California 92093

R. L. Renken and R. L. Sugar
Department of Physics, University of California, Santa Barbara, California 93016

D. Toussaint
Fermi National Accelerator Laboratory, P.O. Box 500, Batavia, Illinois 60510
and Department of Physics, University of California, La Jolla, California 92093
(Received 9 June 1988)

We study the response of the quark number density to infinitesimal chemical potentials in quantum chromodynamics with two flavors of light quarks. We find that both the singlet and nonsinglet susceptibilities give clear signals for the chiral-symmetry-restoration phase transition. They are large and approximately equal in the high-temperature phase, which is consistent with a plasma of light-mass quarks. The quark-number susceptibility is consistent with zero in the low-temperature phase as expected from confinement. For U(1) lattice gauge theory with four flavors of fermions we find that the singlet susceptibility is zero in both the chiral-symmetric and broken phases as expected on theoretical grounds, while the nonsinglet susceptibility jumps at the phase transition.

I. INTRODUCTION

Recently, considerable effort has gone into the study of the chiral-symmetry-restoration phase transition in lattice QCD with dynamical quarks. This transition is important for understanding the structure of the theory and may also have implications for the study of heavy-ion collisions and the early Universe. Simulations by a number of groups[1-5] have shown that for sufficiently light quark masses there is a first-order transition between a low-temperature phase of ordinary hadronic matter in which chiral symmetry is spontaneously broken, and a high-temperature phase in which chiral symmetry is restored. The temperature of this transition has been estimated to be 130 ± 30 MeV for two flavors of zero-mass quarks.[6]

The primary evidence for the restoration of chiral symmetry in the high-temperature phase is the vanishing of $\bar{\psi}\psi$ as the quark mass tends toward zero. Additional evidence comes from measurements of the hadronic screening lengths.[7,8] Here one measures the correlation functions associated with color-singlet quark-antiquark or three-quark sources for large spatial separations. On symmetric (zero-temperature) lattices the exponential falloff of these correlation functions determines the hadron masses. On asymmetric (high-temperature) lattices it determines the hadronic screening lengths. These screening lengths exhibit the parity doubling expected in a chirally symmetric state. In particular, the screening length of the correlation function whose source has the quantum numbers of the nucleon is equal to that of its opposite-parity partner. The inverse screening lengths are comparable in magnitude to the zero-temperature masses. Similarly the π and ρ screening lengths are parity doubled with the σ and a_1 screening lengths, respectively. Explicit chiral symmetry requires a number of relations among the correlation functions themselves, which are found to be well satisfied in the high-temperature phase in the limit of zero quark mass.[8]

It is important to explore the high-temperature phase in greater detail. This phase is often referred to as a quark-gluon plasma. However, at the energy scale of the phase transition the gauge coupling is not small, so the plasma would have to be strongly interacting immediately above the transition temperature. Indeed, the energy density, which jumps at the phase transition, is large in the high-temperature phase and is even larger than the Stefan-Boltzmann law on the lattice.[5] On the other hand, the pressure, which on general grounds must be continuous across the transition, is small in both phases. As a result, the energy and pressure do not satisfy the $P=\frac{1}{3}E$ relationship characteristic of a free relativistic gas. It has been suggested[9] that the long-distance behavior of the high-temperature phase is characterized by the propagation of color-singlet objects, just as in the low-temperature phase.

Additional information concerning the high-temperature phase can be obtained by studying the response of the quark number density to changes in the chemical potential.[10,11] We are at present performing simulations of QCD with two flavors of light dynamical quarks: the u and d. The expectation values of the number density of u and d quarks, n_u and n_d, are given by

$$n_u=\frac{1}{V_s\beta}\frac{\partial}{\partial\mu_u}\ln Z\ , \tag{1}$$

$$n_d = \frac{1}{V_s \beta} \frac{\partial}{\partial \mu_d} \ln Z \ , \tag{2}$$

where V_s is the spatial volume, β the inverse temperature, μ_u and μ_d the chemical potentials of the u and d quarks, and Z the partition function. The response of the quark number density to infinitesimal changes in the chemical potential is measured by the singlet susceptibility

$$\chi_S = \left[\frac{\partial}{\partial \mu_u} + \frac{\partial}{\partial \mu_d} \right] (n_u + n_d) \ , \tag{3}$$

while the response of the third component of isospin density is measured by the nonsinglet susceptibility

$$\chi_{\rm NS} = \left[\frac{\partial}{\partial \mu_u} - \frac{\partial}{\partial \mu_d} \right] (n_u - n_d) \ . \tag{4}$$

In the continuum theory, the flavor singlet and nonsinglet susceptibilities appear in the Lagrangian as

$$L = L_0 + \bar{\psi} \gamma_0 (\mu_S + \boldsymbol{\mu}_{\rm NS} \cdot \boldsymbol{\tau}) \psi \ , \tag{5}$$

where ψ is an isospin doublet of the u and d quarks and $\boldsymbol{\tau}$ are the isospin generators. A nonzero $\mu_{\rm NS}$ causes different densities of u and d quarks, and so to completely simulate an environment such as the interior of a neutron star we would need both μ_S and $\mu_{\rm NS}$ nonzero. (Even heavy-ion collisions would have a small $\mu_{\rm NS}$.)

It is notoriously difficult to perform QCD simulations at finite singlet chemical potential; however, these susceptibilities can be measured at zero chemical potential in a standard QCD simulation, just as the magnetic susceptibility of a ferromagnet can be measured from the fluctuations in the magnetization at zero external field. The measurement procedure will be discussed in detail in Sec. II.

In order to understand the type of information that can be obtained from the susceptibilities, consider a gas of free quarks. If the quark mass is small, then we expect both χ_S and $\chi_{\rm NS}$ to be large since it is relatively easy to create a quark or antiquark. For example, if the quark mass m is much smaller than the temperature T then in the continuum limit $\chi_S \to N_f T^2$, where N_f is the number of quark flavors. On the other hand, if the quarks are massive then it will be difficult to create a quark or antiquark, and the susceptibilities will be suppressed by a factor of $\exp(-m/T)$. As we have already indicated, the high-temperature phase of QCD is unlikely to be described in terms of a gas of free quarks in the vicinity of the transition temperature. Nevertheless, if the fundamental excitations of the system are low-mass objects with the quantum numbers of quarks, then we expect both χ_S and $\chi_{\rm NS}$ to be large. On the other hand, in the low-temperature phase we expect χ_S to be small since quarks are confined and the only states with nonzero quark number have large masses. However, $\chi_{\rm NS}$ can be large in the low-temperature phase since the isospin-one pion is the lowest-mass state in this phase.

The baryon-number susceptibility may be important in understanding the history of the early Universe. In particular, if the two phases of QCD have very different susceptibilities and if the transition is first order with large supercooling, the chiral-symmetry-breaking phase transition could cause inhomogeneities in the baryon density which might survive to affect nucleosynthesis.[12]

The organization of the paper is as follows. In Sec. II we describe in detail our procedure for evaluating the fermion-number susceptibilities. In Sec. III we present numerical data for both SU(3) and U(1) lattice gauge theory with dynamical fermions, and briefly discuss our results. Finally in an appendix we discuss the susceptibility of a free fermion gas on the lattice. As is well known, care must be taken in introducing a chemical potential into lattice theories in order to obtain a finite result in the continuum limit.[13,14] We show that the prescription obtained by Gavai[13] for the finiteness of the energy density for nonzero μ is sufficient to ensure the finiteness of the quark-number susceptibility.

II. FERMION-NUMBER SUSCEPTIBILITY ON THE LATTICE

Let us begin by discussing the fermion-number susceptibilities in the continuum theory for two flavors of fermions. After integrating out the fermion degrees of freedom the partition function can be written as

$$\begin{aligned} Z &= \int [\delta U] e^{-S_g} \det M_u(U, \mu_u) \det M_d(U, \mu_d) \\ &\equiv \int [\delta U] e^{-S_{\rm eff}(U, \mu_u, \mu_d)} \ . \end{aligned} \tag{6}$$

Here S_g is the action for the pure gauge theory, U is the gauge field, and $M_{u,d}$ and $\mu_{u,d}$ are, respectively, the fermion matrices (inverse propagators) and chemical potentials of the two flavors of fermions, which we have denoted by u and d. $[\delta U]$ denotes an integration over all configurations of the gauge field. Equations (1) and (2) can be rewritten in the form

$$\begin{aligned} n_\alpha &= Z^{-1} \int [\delta U] e^{-S_{\rm eff}} (V_s \beta)^{-1} {\rm Tr} \left[\frac{1}{M_\alpha} \frac{\partial M_\alpha}{\partial \mu_\alpha} \right] \\ &\equiv (V_s \beta)^{-1} \left\langle {\rm Tr} \left[\frac{1}{M_\alpha} \frac{\partial M_\alpha}{\partial \mu_\alpha} \right] \right\rangle_U \ , \end{aligned} \tag{7}$$

with $\alpha = u, d$. The singlet and nonsinglet susceptibilities are then given by

$$\begin{aligned} \chi_{S,{\rm NS}} = & \frac{1}{V_s \beta} \left\langle {\rm Tr} \left[\sum_{\alpha = u,d} \left[\frac{1}{M_\alpha} \frac{\partial^2 M_\alpha}{\partial \mu_\alpha^2} - \frac{1}{M_\alpha} \frac{\partial M_\alpha}{\partial \mu_\alpha} \frac{1}{M_\alpha} \frac{\partial M_\alpha}{\partial \mu_\alpha} \right] \right] \right\rangle_U \\ & + \frac{1}{V_s \beta} \left\langle \left[{\rm Tr} \left[\frac{1}{M_u} \frac{\partial M_u}{\partial \mu_u} \right] \pm {\rm Tr} \left[\frac{1}{M_d} \frac{\partial M_d}{\partial \mu_d} \right] \right]^2 \right\rangle_U - \frac{1}{V_s \beta} \left\langle {\rm Tr} \left[\frac{1}{M_u} \frac{\partial M_u}{\partial \mu_u} \right] \pm {\rm Tr} \left[\frac{1}{M_d} \frac{\partial M_d}{\partial \mu_d} \right] \right\rangle_U^2 \ , \end{aligned} \tag{8}$$

where the plus signs are for χ_S and the minus signs for $\chi_{\rm NS}$. Since the continuum fermion matrices are linear in the chemical potential the first term on the right-hand side of Eq. (8) naively vanishes. We have included it here because on the lattice the fermion matrices are nonlinear in μ, and such terms play an essential role.

In perturbation theory for equal-mass quarks the contributions to the susceptibilities are represented by the Feynman diagrams in Fig. 1. In these diagrams the dots represent insertions of the baryon number of isospin current. The circled dot in Fig. 1(b) represents the $\partial^2 M/\partial\mu^2$ term in Eq. (8). Only the quark parts of the diagrams are drawn—gluons should be added in all possible ways. Since the nonsinglet susceptibility includes an isospin matrix at every dot, it is clear that the diagram in Fig. 1(c) will not contribute to the nonsinglet susceptibility, and that Figs. 1(a) and 1(b) will contribute equally to the singlet and nonsinglet susceptibilities.

The susceptibility has dimensions of mass squared, and therefore should go as T^2. However, if care is not taken in regularization we are likely to find a term proportional to $1/a^2$, where a is the lattice spacing. In the continuum theory this is handled by simply subtracting the result at zero temperature. In the lattice theory the second derivative term, Fig. 1(b), which arises when both derivatives with respect to μ act on the same link, cancels this divergence. This can be seen by computing the zero-temperature susceptibility of a free fermion theory, as will be discussed further in the Appendix.

For the lattice theory we use staggered fermions, and write the fermion matrix in the form

$$M(U)_{i,j}=2ma\delta_{i,j}+\sum_{\nu=x,y,z}\eta_{i,\nu}(U_{i,\hat{\nu}}\delta_{i,j-\hat{\nu}}-U^{\dagger}_{i-\hat{\nu},\nu}\delta_{i,j+\hat{\nu}})+\eta_{i,t}(U_{i,t}e^{a\mu}\delta_{i,j-\hat{t}}-U^{\dagger}_{i-\hat{t},t}e^{-a\mu}\delta_{i,j+\hat{t}})\ . \tag{9}$$

Here i and j specify lattice sites, $U_{i,\nu}$ is the SU(3) or U(1) matrix associated with the lattice link between sites i and $i+\hat{\nu}$, a is the lattice spacing, and η the standard staggered fermion phases. The prescription for introducing the chemical potential has been discussed by a number of authors.[13,14] In the Appendix we show that the choice made in Eq. (9) is just one of a class that will lead to a finite continuum limit for both the energy density and fermion-number susceptibilities for the free theory.

The staggered fermion matrix given in Eq. (9) describes four flavors of fermions each coupled to an identical chemical potential μ. In order to simulate N_f flavors of light fermions, we can use the effective action

$$S_{\rm eff}=S_W+\frac{N_f}{4}{\rm Tr}\ln M(U,\mu)\ . \tag{10}$$

The factor of $N_f/4$ ensures that the fermion loops are weighted correctly. In our present work we take $N_f=2$, but we will present formulas for the general case. The functional integral of Eq. (6) is, of course, now an integral over all link matrices $U_{i,\nu}$ with the Haar measure.

We can read off expressions for χ_S and $\chi_{\rm NS}$ from Eqs. (8) and (10):

$$\chi_S=\frac{1}{V_s\beta}\frac{N_f}{4}\left[\left\langle{\rm Tr}\frac{1}{M}\frac{\partial^2 M}{\partial\mu^2}\right\rangle_U-\left\langle{\rm Tr}\frac{1}{M}\frac{\partial M}{\partial\mu}\frac{1}{M}\frac{\partial M}{\partial\mu}\right\rangle_U\right]+\frac{1}{V_s\beta}\left[\frac{N_f}{4}\right]^2\left[\left\langle{\rm Tr}\frac{1}{M}\frac{\partial M}{\partial\mu}{\rm Tr}\frac{1}{M}\frac{\partial M}{\partial\mu}\right\rangle_U-\left\langle{\rm Tr}\frac{1}{M}\frac{\partial M}{\partial\mu}\right\rangle_U^2\right] \tag{11}$$

and

$$\chi_{\rm NS}=\frac{1}{V_s\beta}\frac{N_f}{4}\left[\left\langle{\rm Tr}\frac{1}{M}\frac{\partial^2 M}{\partial\mu^2}\right\rangle_U-\left\langle{\rm Tr}\frac{1}{M}\frac{\partial M}{\partial\mu}\frac{1}{M}\frac{\partial M}{\partial\mu}\right\rangle_U\right]\ . \tag{12}$$

Again $\langle\ \rangle_U$ denotes an average over gauge configurations weighted as $\exp(-S_{\rm eff})$. It is, of course, extremely difficult to generate such configurations for $\mu\neq 0$, since the fermion determinant, and therefore the effective action, are not real. However, we can determine χ_S and $\chi_{\rm NS}$ at $\mu=0$ by means of a standard simulation, and thereby determine the response of the system to infinitesimal changes in the chemical potentials.

In order to gain some insight into the structure of the susceptibilities, let us imagine making a loop expansion of the fermion determinant. On a finite lattice there are a finite number of terms in such an expansion. Ordinary closed loops will be independent of the chemical potential

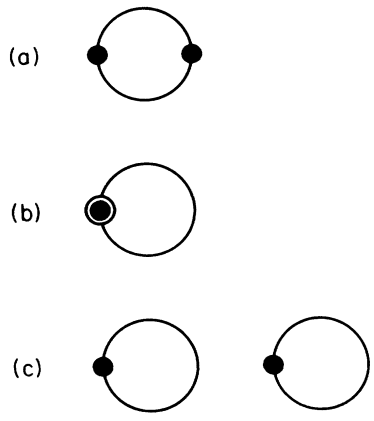

FIG. 1. Feynman diagrams contributing to the susceptibilities for equal-mass quarks. The dots represent insertions of the baryon number or isospin current. The circled dot in (b) represents the $\partial^2 M/\partial\mu^2$ term in Eq. (8). Only the quark parts of the diagrams are shown.

since they will have as many links directed in the forward as backward time direction—that is as many factors of $\exp(a\mu)$ as of $\exp(-a\mu)$. The μ dependence of the partition function will come from loops that wind one or more times around the lattice in the Euclidean time direction. At $\mu=0$ the contribution to $\partial \ln Z/\partial\mu$ arising from a single gauge configuration will have the form

$$\mathrm{Tr}\frac{1}{M}\frac{\partial M}{\partial\mu}=\sum_L C_L(U,U^\dagger)\mathrm{Tr}(U_L-U_L^\dagger)\ . \tag{13}$$

U_L is a product of U matrices along a path L that winds one or more times around the lattice in the Euclidean time direction. The sum in Eq. (13) is over all such paths. The terms proportional to U_L and $U_L^\dagger$ correspond to the two possible ways of traversing these paths. The fact that they enter with opposite signs follows from the way the chemical potential enters into Eq. (9). The coefficients $C_L(U,U^\dagger)$ arise from products of loops that are not differentiated. Taking into account that there are two ways of traversing such loops, one sees that for $\mu=0$ the C_L are real and symmetric under interchange of U and $U^\dagger$. Thus, it is clear that for any particular gauge configuration $\mathrm{Tr}(1/M)(\partial M/\partial\mu)$ is pure imaginary, which reflects the fact that the effective action becomes complex for nonzero values of the chemical potential. The average of $\mathrm{Tr}(1/M)(\partial M/\partial\mu)$ over all gauge configurations vanishes since it changes sign under the transformation $U\rightarrow U^\dagger$, while the Wilson action and the measure are invariant. Notice that the third term on the right-hand side of Eq. (11) does not vanish. It makes a negative contribution to χ_S. This gives the inequality $\chi_{\mathrm{NS}}\geq\chi_S$. In the low-temperature phase, this inequality reflects the existence of mesons which have isospin but no baryon number and so contribute to χ_{NS} but not to χ_S.

In a quenched approximation calculation there is no mechanism for the density of one flavor of quark to affect the density of another, so $\partial n_u/\partial\mu_d=0$. Therefore, from Eqs. (3) and (4), in the quenched approximation $\chi_S=\chi_{\mathrm{NS}}$. This is related to the fact that in quenched approximation calculations with finite chemical potential at zero temperature the condensate appears to form at $\mu=\frac{1}{2}m_\pi$ rather than at $\mu=\frac{1}{3}m_N$ (Ref. 15).

The simulation is carried out at zero chemical potential with the effective action of Eq. (10). Independent configurations of the gauge fields are generated using the hybrid molecular-dynamics algorithm that we have previously described in detail.[16,17] The measurement of the susceptibilities poses a major difficulty. The exact evaluation of the traces in Eqs. (11) and (12) would be prohibitively expensive since it would require a computation of all of the matrix elements of M^{-1}. By contrast in generating new field configurations and in most measurements it is only necessary to calculate M^{-1} applied to a particular vector, and this can be done relatively effectively by the conjugate-gradient method. To remedy this situation we make use of unbiased estimators for χ_S and χ_{NS}. We introduce L vectors of complex Gaussian random numbers R_α, $\alpha=1,\ldots,L$, of dimension equal to the lattice volume. The individual components of R_α, $R_{\alpha,i}$, are distributed as $\exp(-|R_{\alpha,i}|^2)$. We then have the identities

$$\left\langle R_\alpha^\dagger\frac{1}{M}\frac{\partial M}{\partial\mu}R_\alpha\right\rangle_R=\mathrm{Tr}\frac{1}{M}\frac{\partial M}{\partial\mu} \tag{14}$$

and

$$\left\langle R_\alpha^\dagger\frac{1}{M}\frac{\partial M}{\partial\mu}R_\alpha R_\beta^\dagger\frac{1}{M}\frac{\partial M}{\partial\mu}R_\beta\right\rangle_R=\left[\mathrm{Tr}\frac{1}{M}\frac{\partial M}{\partial\mu}\right]^2+\delta_{\alpha,\beta}\mathrm{Tr}\left[\frac{1}{M}\frac{\partial M}{\partial\mu}\right]^2, \tag{15}$$

where $\langle\ \rangle_R$ indicates an average over the Gaussian random vectors. The susceptibilities can now be obtained by averaging over both the gauge configurations U and the random vectors R:

$$\chi_S=\frac{1}{V_s\beta}\frac{N_f}{4}\left[\left\langle R_1^\dagger\frac{1}{M}\frac{\partial^2 M}{\partial\mu^2}R_1\right\rangle_{U,R}-\left[1+\frac{N_f}{4}\frac{1}{L}\right]\left\langle R_1^\dagger\frac{1}{M}\frac{\partial M}{\partial\mu}\frac{1}{M}\frac{\partial M}{\partial\mu}R_1\right\rangle_{U,R}\right]$$
$$+\frac{1}{V_s\beta}\left[\frac{N_f}{4}\frac{1}{L}\right]^2\left\langle\sum_{\alpha,\beta=1}^{L}R_\alpha^\dagger\frac{1}{M}\frac{\partial M}{\partial\mu}R_\alpha R_\beta^\dagger\frac{1}{M}\frac{\partial M}{\partial\mu}R_\beta\right\rangle_{U,R} \tag{16}$$

and

$$\chi_{\mathrm{NS}}=\frac{1}{V_s\beta}\frac{N_f}{4}\left[\left\langle R_1^\dagger\frac{1}{M}\frac{\partial^2 M}{\partial\mu^2}R_1\right\rangle_{U,R}-\left\langle R_1^\dagger\frac{1}{M}\frac{\partial M}{\partial\mu}\frac{1}{M}\frac{\partial M}{\partial\mu}R_1\right\rangle_{U,R}\right]. \tag{17}$$

The third term in Eq. (16), which gives rise to the two-trace term in Eq. (11), has a significantly larger variance than the terms quadratic in R_α. It is advantageous to use a number of random vectors at each measurement of this term even though this introduces extra conjugate-gradient calculations. With L random vectors we obtain L^2 estimates of the two-trace term. The variance of this term for a single gauge configuration is given by

$$V_2=\left\langle\left[\frac{1}{L}\sum_{\alpha=1}^{L}R_\alpha^\dagger\frac{1}{M}\frac{\partial M}{\partial\mu}R_\alpha\right]^4\right\rangle_R-\left\langle\left[\frac{1}{L}\sum_{\alpha=1}^{L}R_\alpha^\dagger\frac{1}{M}\frac{\partial M}{\partial\mu}R_\alpha\right]^2\right\rangle_R^2$$
$$=\frac{4}{L}\left[\mathrm{Tr}\frac{1}{M}\frac{\partial M}{\partial\mu}\right]^2\mathrm{Tr}\left[\frac{1}{M}\frac{\partial M}{\partial\mu}\right]^2+\frac{2}{L^2}\left[\mathrm{Tr}\left[\frac{1}{M}\frac{\partial M}{\partial\mu}\right]^2\right]^2+\frac{8}{L^2}\mathrm{Tr}\frac{1}{M}\frac{\partial M}{\partial\mu}\mathrm{Tr}\left[\frac{1}{M}\frac{\partial M}{\partial\mu}\right]^3+\frac{6}{L^3}\mathrm{Tr}\left[\frac{1}{M}\frac{\partial M}{\partial\mu}\right]^4. \quad (18)$$

For large values of L the variance will of course fall as $1/L$. However, $[\mathrm{Tr}(1/M)(\partial M/\partial\mu)]^2$, which appears in the $1/L$ term in Eq. (18), is generally small compared to $\mathrm{Tr}[(1/M)(\partial M/\partial\mu)]^2$. Therefore, for intermediate values of L such that

$$L\ll\mathrm{Tr}\left[\frac{1}{M}\frac{\partial M}{\partial\mu}\right]^2\Big/\left[\mathrm{Tr}\frac{1}{M}\frac{\partial M}{\partial\mu}\right]^2, \quad (19)$$

the variance will fall like $1/L^2$ with increasing L. Since each additional random vector requires an additional conjugate-gradient calculation, the size of the error bars will be inversely proportional to the computer time in such a regime. We have typically used $L=10$, and found that in the neighborhood of this value the variance of the two-trace term is proportional to $1/L^2$.

III. NUMERICAL RESULTS

We first discuss results for SU(3) lattice gauge theory with two flavors of dynamical quarks. We have previously reported calculations of the quark-number susceptibilities on $8^3\times4$ lattices with $am=0.05$. Here we present results for $am=0.025$ on $8^3\times4$ and $10^3\times6$ lattices.

In Figs. 1 and 2 we plot χ_S and χ_{NS} as a function of $6/g^2$ for the $8^3\times4$ lattice. We have measured the critical coupling for the transition between the chiral-symmetric and broken-symmetry phases to be $6/g_c^2=5.28\pm0.01$ for this lattice and quark mass.[18] This point is marked by the arrow labeled T_c in the figures. We have found the critical coupling for the $10^3\times6$ lattice to be $6/g_c^2=5.43\pm0.03$. This value corresponds to a temperature of $1.5T_c$ on the present lattice and has been so marked in the figures. We see that χ_S is consistent with zero in the low-temperature phase, as is expected from confinement. In this phase all states with nonzero quark number have large masses. In addition, χ_{NS} is small in the low-temperature phase. In this case the lowest excitation is expected to be the pion. We have measured the pion mass on an $8^3\times24$ lattice at $6/g^2=5.28$, and found $am_\pi=0.4184\pm0.0009$ (Ref. 18). Since $T_c=1/4a\approx130$ MeV (Ref. 6) we have $m_\pi\approx218$ MeV. As χ_{NS} will be proportional to $\exp(-m_\pi/T)$ at low temperatures, it is hardly surprising to see a suppression for $T<T_c$. Both χ_S and χ_{NS} rise sharply as the temperature is increased through its critical value indicating that the fundamental excitations in the high-temperature phase have small free energy. The fact that the two susceptibilities approach approximately the same limit is consistent with these excitations being light-mass quarks. Using the same argument as for the pion, the bare-quark mass is approximately 13 MeV, which is small on the scale of T_c.

The increase in χ_{NS} across the transition can in part be explained by the difference in weight of the quark and pion states. For zero chemical potential $\chi_{\mathrm{NS}}=\langle I_z^2\rangle$, where I_z is the z component of isotopic spin. (The scaling of χ as the square of the isospin or baryon number of the particle is easily understood. For example, since the baryon number of a nucleon is 3 times that of a quark, 3 times as much energy is gained by adding a baryon to the system, and each baryon added contributes 3 times as much to the charge as a quark.) There are three pion states, two with $I_z^2=1$, and one with $I_z^2=0$. Taking into account the color, spin, isospin, and particle-antiparticle degrees of freedom, we have 24 quark states each with $I_z^2=\frac{1}{4}$, so the quark states have 3 times the weight of the one-pion states. Similarly, at zero chemical potential χ_S measures the square of the quark number. Single nucleon states will contribute to χ_S with 3 times the weight of single-quark states. It has been pointed out that because of the large statistical weight of the baryon states, the excitation of many such states at high temperatures would give rise to an increase in the susceptibilities. However, this effect is not expected to give as sharp a transition as we have found.[19] In addition, comparing the present results with our previous ones at $am=0.05$, one finds a significant sharpening of the crossover as the quark mass is lowered. It is difficult to explain such behavior in terms of color-singlet baryon states, whose masses are rel-

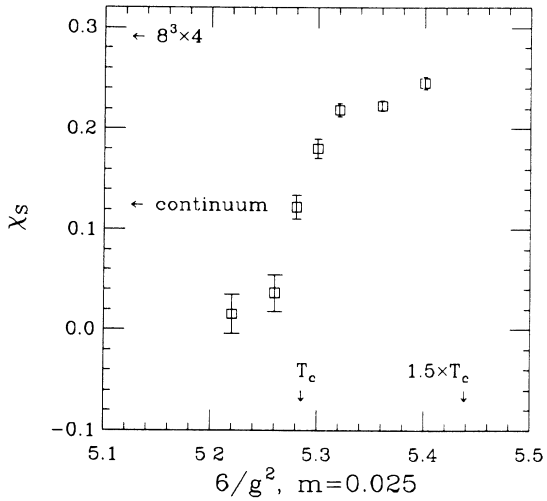

FIG. 2. χ_S as a function of $1/g^2$ for quark mass of 0.025 on an $8^3\times4$ lattice. The horizontal arrows label the values of χ_S for two flavors of free quarks of this mass on an $8^3\times4$ lattice and in the continuum. The vertical arrows indicate our earlier estimates of the values of $1/g^2$ at which the high-temperature crossover occurs for $N_T=4$ and 6. This may be interpreted as the crossover temperature and 1.5 times the crossover tempera-

atively insensitive to the quark mass in this parameter region.[18] Furthermore the apparent equality of χ_S and χ_{NS} is most easily explained if the fundamental excitations in the high-temperature phase are quarks.

The cancellation between the two one-trace diagrams [Figs. 1(a) and 1(b)] is essential to our results. For $am_q=0.025$ on the $8^3\times4$ lattice at $6/g^2=5.36$, in the high-temperature phase the two diagrams contribute $-0.183(2)$ and $0.414(7)$, respectively, giving $\chi_{NS}=0.231(2)$. In the low-temperature phase at $6/g^2=5.22$ the two terms are $-0.351(5)$ and $0.378(1)$, for a total of $0.027(5)$.

We have calculated susceptibilities for a gas of free quarks by summing modes in momentum space, and the results are marked by arrows in Figs. 1 and 2 for both an $8^3\times4$ lattice and for the continuum limit. It is clear that there are very significant finite-size effects on the lattices we are studying. Of course, the quark interactions are not small in the coupling range under consideration, and we are not dealing with a gas of free quarks.

In the low-temperature phase, χ_S has significantly larger error bars than χ_{NS} because of fluctuations in the two-trace term. In Fig. 4 we plot $\chi_S-\chi_{NS}$, which measures the response of n_u to a change in μ_d. Although this difference is small and the error bars relatively large, it is clearly negative. In Fig. 5 we plot $\langle\bar{\psi}\psi\rangle$ as a function of $6/g^2$ for the same lattice and quark mass. The crossover occurs at the same coupling as for the susceptibilities. Indeed, χ_S and χ_{NS} provide as good a signal for the phase transition as $\langle\bar{\psi}\psi\rangle$.

In Figs. 6 and 7 we present data for χ_S and χ_{NS} on a $10^3\times6$ lattice. The critical value of $6/g^2$ is marked by the arrow labeled T_c. The critical value of $6/g^2$ for the $8^3\times4$ lattice corresponds to a temperature of $\frac{2}{3}T_c$ and labeled accordingly. The qualitative results are the same as those found for the $8^3\times4$ lattice, although the statistical errors are larger.

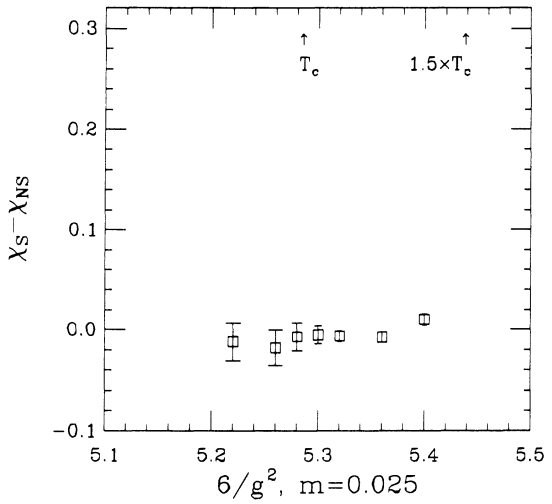

FIG. 4. $\chi_S-\chi_{NS}$ as a function of $1/g^2$ for quark mass of 0.025 on an $8^3\times4$ lattice. This quantity is the two-trace term in Eq. (10).

Kogut and Dagotto have recently provided convincing evidence that compact U(1) lattice gauge theory with four flavors of dynamical fermions has a first-order phase transition between a phase in which chiral symmetry is spontaneously broken and one in which it is realized.[20] We have measured χ_S and χ_{NS} for two values of $6/g^2$ in each of these phases. The results are shown in Fig. 8 with the data for χ_S being plotted as squares and that for χ_{NS} as circles. Note that χ_{NS} changes dramatically across the phase transition, while χ_S is consistent with zero in both phases.

We can understand the vanishing of χ_S in two ways. First, if we set the chemical potentials of all fermions equal as is appropriate for a measurement of χ_S, then the chemical potential is coupled to the total charge, which is

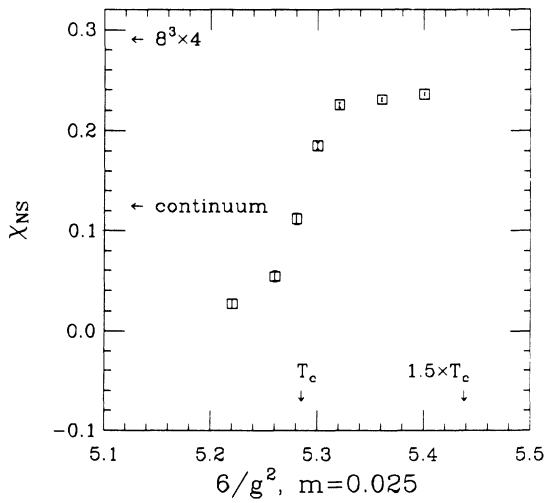

FIG. 3. χ_{NS} as a function of $1/g^2$ for quark mass of 0.025 on an $8^3\times4$ lattice.

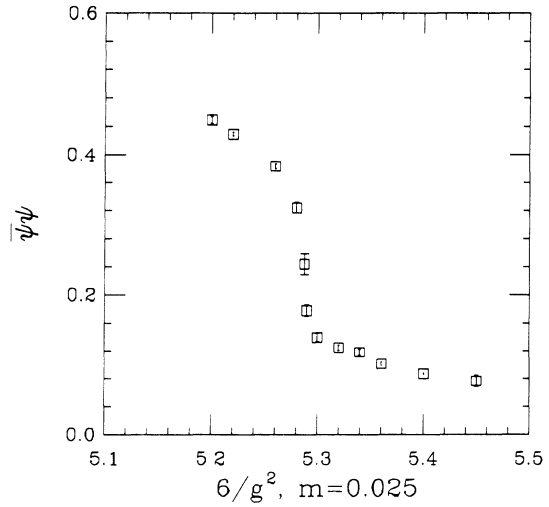

FIG. 5. $\psi\bar{\psi}$ as a function of $1/g^2$ for $m=0.025$ on an $8^3\times4$ lattice.

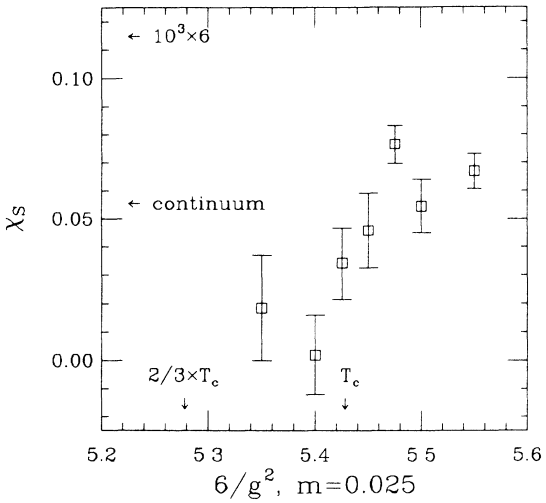

FIG. 6. χ_S as a function of $1/g^2$ for quark mass of 0.025 on a $10^3\times6$ lattice.

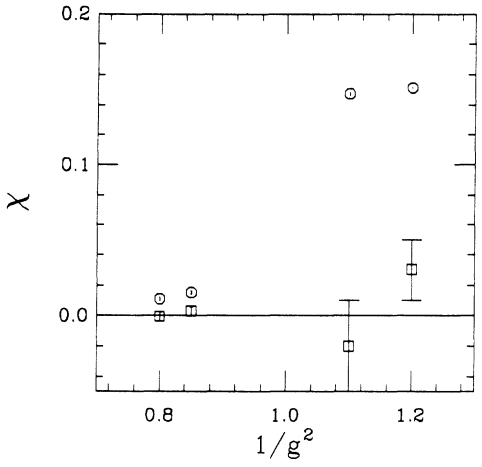

FIG. 8. χ_S and χ_{NS} for U(1) lattice gauge theory with a quark mass of 0.25 on a $8^3\times4$ lattice. The squares are χ_S and the circles χ_{NS}.

the generator of the gauge symmetry. There is a long-range field associated with this charge. So, if we try to put a finite charge in a periodic box there is nowhere for the flux to go. This situation is quite different from SU(3) lattice gauge theory, where the quark number is not a generator of the gauge symmetry, and is therefore not associated with a long-range field. The same result can be understood from a loop expansion of the fermion determinant. As we pointed out previously, the only terms in this expansion that depend on the chemical potential are those arising from loops that wind around the lattice one or more times in the Euclidean time direction. Suppose we make a transformation for all temporal links emanating from a single time slice of the form $U\rightarrow Ue^{i\theta}$. The pure gauge action will be invariant under such a transformation, but a temporal loop that winds around the lattice N times will pick up a factor of $\exp(i\theta N)$. Clearly such a term will average to zero when we integrate over all gauge configurations. So, the partition function will be independent of the chemical potential and χ_S will vanish identically.[15] This argument clearly does not hold when the chemical potentials of the individual fermions are not equal, so χ_{NS} need not vanish. For SU(3) lattice gauge theory, the argument goes through for transformations generated by the center of the group, Z_3. In this case, we see that χ_S need not vanish, but receives contributions only from temporal loops with winding numbers that are multiples of 3. The fact that the overall quark number must be a multiple of 3 does not imply that the quarks are confined—they might be arbitrarily far apart.

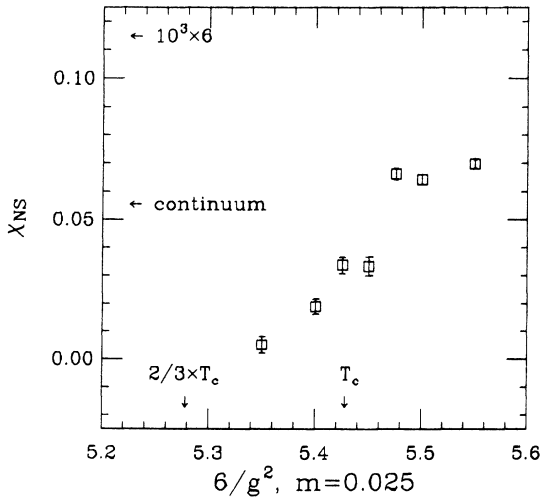

FIG. 7. χ_{NS} as a function of $1/g^2$ for quark mass of 0.025 on a $10^3\times6$ lattice.

The large value of χ_{NS} in the chiral-symmetric phase is analogous to the results found for SU(3) lattice gauge theory. Our interpretation is that the fundamental excitations in this phase are the light-mass electrons, associated with the fundamental fermion fields in the theory. The small value of χ_{NS} in the broken symmetry phase indicates that as in the case of SU(3) the fundamental excitations in this phase are massive bound states.

We believe that our results for SU(3) and U(1) gauge theories indicate that the quark-number susceptibilities are useful tools for locating chiral-symmetry-restoration phase transitions and for exploring the properties of the different phases.

ACKNOWLEDGMENTS

We thank C. DeTar, G. Fuller, A Gocksch, L. McLerran, and P. Rossi for helpful discussions and comments. This work was supported in part by National Science Foundation Grants Nos. PHY-86-14185 and DMR83-20423, and by Department of Energy Grants Nos. DE-AT03-81ER40029 and DE-AC02-84ER-40125. D.T.

thanks the Alfred P. Sloan Foundation for financial support.

APPENDIX

Care must be taken in introducing a chemical potential into lattice field theories. This problem has been studied in detail for free fermions,[13,14] and Gavai has obtained a set of constraints that must be satisfied if the energy density is to have a finite continuum limit.[13] In this appendix we show that these constraints are sufficient to guarantee that the quark number density and susceptibilities also have finite continuum limits.

We present our discussion for the case of naive fermions. The extension to staggered fermions merely requires the introduction of projection operators. Following the notation of Gavai we write the fermion matrix in the form

$$M_{i,j}=ma\delta_{i,j}+\tfrac{1}{2}\sum_{\nu=x,y,z}\gamma_\nu(\delta_{i,j-\nu}-\delta_{i,j+\nu}) +\tfrac{1}{2}\gamma_0[f(a\mu)\delta_{i,j-\hat{\imath}}-g(a\mu)\delta_{i,j+\hat{\imath}}] , \tag{A1}$$

where γ_μ are the standard Euclidean Dirac matrices. Gavai has found that one can obtain the correct continuum limit for the energy density at finite chemical potential provided $f(a\mu)g(a\mu)=1$ and $\lim_{a\to 0}f(a\mu)-g(a\mu)\sim 2a\mu$. It is convenient to write

$$\tfrac{1}{2}(f+g)=R\cosh\theta,\quad \tfrac{1}{2}(f-g)=R\sinh\theta . \tag{A2}$$

Gavai's finiteness conditions then become $R=1$ and $\theta\lim_{a\to 0}a\mu$.

For free fermions the fermion matrix can be diagonalized in momentum space:

$$M(p)=i\gamma\cdot\mathbf{P}+i\gamma_0 R\sin(p_0a+i\theta) , \tag{A3}$$

with

$$\mathbf{P}=(\sin p_x a,\sin p_y a,\sin p_z a) , \tag{A4}$$

$$p_i a=2\pi n_i/N , \tag{A5}$$

and

$$p_0 a=2\pi(n_0+\tfrac{1}{2})/L . \tag{A6}$$

Here N and L are the number of lattice points in the space and time directions, respectively, and $n_i,n_0=0,\pm1,\pm2,\ldots$. Let us begin by considering the expectation value of the number density:

$$\langle n\rangle=\frac{1}{V_s\beta}\sum_{\mathbf{n},n_0}\mathrm{Tr}\left[\frac{1}{M(p)}\frac{\partial M(p)}{\partial\mu}\right]$$

$$=\frac{4}{V_s\beta}\sum_{\mathbf{n},n_0}\frac{1}{\epsilon^2+R^2\sin^2(p_0a+i\theta)} \times\left[iR\frac{\partial\theta}{\partial\mu}\sin(p_0+i\theta)\cos(p_0+i\theta) +\frac{\partial R}{\partial\mu}\sin^2(p_0a+i\theta)\right] , \tag{A7}$$

with $\epsilon=[\mathbf{P}^2+(am)^2]^{1/2}$.

We go to the zero temperature by taking $L\to\infty$ for fixed a. The sum over n_0 becomes an integral, and we have

$$\langle n\rangle=\frac{4}{V_s}\sum_{\mathbf{n}}\int_{-\pi}^{\pi}\frac{dp_0}{2\pi}\frac{1}{\epsilon^2+R^2\sin^2(p_0a+i\theta)} \times\left[iR\frac{\partial\theta}{\partial\mu}\sin(p_0+i\theta)\cos(p_0+i\theta) +\frac{\partial R}{\partial\mu}\sin^2(p_0a+i\theta)\right] . \tag{A8}$$

To evaluate the integral over p_0 it is convenient to make the change of variable $z=\exp(ip_0)$. We then have a contour integral around the unit circle in the complex z plane. The integrand has poles at $z=0$ and at $z=\pm z_+$, where

$$z_\pm=e^\theta\{[(\epsilon/R)^2+1]^{1/2}\pm\epsilon/R\} . \tag{A9}$$

For definiteness we take $\theta>0$. Then the poles at $z=\pm z_-$ are inside the unit circle for $\epsilon>R\sinh\theta$, while those at $z=\pm z_+$ are never inside the unit circle. The contour integral can be done straightforwardly. For $\epsilon>R\sinh\theta$ the residue of the pole at $z=0$ exactly cancels those of the poles at $z=\pm z_-$. We find

$$\langle n\rangle=\frac{4}{V_s}\sum_{\mathbf{n}}\left[\frac{1}{R}\frac{\partial\theta}{\partial(a\mu)}\vartheta(R\sinh\theta-\epsilon)+\frac{1}{R^2}\frac{\partial R}{\partial(a\mu)}\left[1-\frac{\epsilon}{(\epsilon^2+R^2)^{1/2}}\vartheta(\epsilon-R\sinh\theta)\right]\right] . \tag{A10}$$

ϑ is the standard step function. If we now approach the continuum limit by letting $a\to 0$ and $V_s\to\infty$, then the term in Eq. (A10) proportional to $\partial R/\partial(a\mu)$ will give rise to ultraviolet divergences. We must therefore take R to be independent of $a\mu$. On the other hand, in order to obtain the correct continuum limit we must have $\lim_{a\to 0}R=1$ and $\lim_{a\to 0}\theta\sim a\mu$, as is true for the calculation of the energy density. With these restrictions we obtain in the continuum limit

$$\langle n\rangle=4\int\frac{d^3p}{(2\pi)^3}\vartheta(\mu-(p^2+m^2)^{1/2}) . \tag{A11}$$

The factor of 4, of course, indicates that the naive fermion matrix describes four species of fermions.

For free fermions $\chi_S = \chi_{NS}$. The susceptibilities can be obtained by simply differentiating the above formulas with respect to μ.

Alternatively, the $\mathrm{Tr}[(1/M)(\partial M/\partial\mu)(1/M)(\partial M/\partial\mu)]$ term [Fig. 1(a)] and the $\mathrm{Tr}[(1/M)(\partial^2 M/\partial\mu^2)]$ term [Fig. 1(b)] in the susceptibility can be evaluated separately by similar means. If this is done it can be seen that each diagram is nonzero at $T=0$ and hence divergent, but the divergences cancel between the two diagrams. [Figure 1(c) does not contribute for free fermions.]

[1]M. Fukugita and A. Ukawa Phys. Rev. Lett. **57**, 503 (1986); M. Fukugita, S. Ohta, Y. Oyanagi, and A. Ukawa, *ibid.* **58**, 2515 (1987).

[2]E. V. E. Kovacs, D. K. Sinclair, and J. B. Kogut, Phys. Rev. Lett. **58**, 751 (1987); F. Karsch, J. B. Kogut, D. K. Sinclair, and H. W. Wyld, Phys. Lett. B **188**, 353 (1987).

[3]R. Gupta, G. Guralnik, G. W. Kilcup, A. Patel, and S. R. Sharpe, Phys. Rev. Lett. **57**, 2621 (1986).

[4]R. V. Gavai, J. Potvin, and S. Sanielevici, Phys. Rev. Lett. **58**, 2519 (1987).

[5]S. Gottlieb, W. Liu, D. Toussaint, R. L. Renken, and R. L. Sugar, Phys. Rev. D **35**, 3972 (1987).

[6]S. Gottlieb, W. Liu, D. Toussaint, R. L. Renken, and R. L. Sugar, Phys. Rev. Lett. **59**, 1513 (1987).

[7]C. DeTar and J. Kogut, Phys. Rev. Lett. **59**, 399 (1987); Phys. Rev. D **36**, 2828 (1987).

[8]S. Gottlieb, W. Liu, D. Toussaint, R. L. Renken, and R. L. Sugar, Phys. Rev. Lett. **59**, 2247 (1987).

[9]C. DeTar, Phys. Rev. D **32**, 276 (1985); T. A. DeGrand, and C. DeTar, *ibid.* **34**, 2469 (1986).

[10]S. Gottlieb, W. Liu, D. Toussaint, R. L. Renken, and R. L. Sugar, Phys. Rev. Lett. **59**, 2247 (1987).

[11]L. McLerran, Phys. Rev. D **36**, 3291 (1987).

[12]K. E. Sale and G. J. Mathews, Astrophys. J. **309**, L1 (1986); J. H. Applegate, C. J. Hogan, and R. J. Scherrer, Phys. Rev. D **35**, 1151 (1987); C. A. Alcock, G. M. Fuller, and G. J. Mathews, Astrophys. J. **320**, 439 (1987).

[13]R. V. Gavai, Phys. Rev. D **32**, 519 (1985).

[14]J. Kogut, H. Matsuoka, M. Stone, H. W. Wyld, S. Shenker, J. Shigemitsu, and D. K. Sinclair, Nucl. Phys. **B225**, 93 (1983); P. Hasenfratz and F. Karsch, Phys. Lett. **125B**, 308 (1983).

[15]I. Barbour, N. Bihilil, E. Dagotto, F. Karsch, A. Moreo, M. Stone, and H. W. Wyld, Nucl. Phys. **B275** [FS17], 296 (1986).

[16]S. Gottlieb, W. Liu, D. Toussaint, R. L. Renken, and R. L. Sugar, Phys. Rev. D **35**, 2531 (1987).

[17]S. Gottlieb, W. Liu, D. Toussaint, R. L. Renken, and R. L. Sugar, Phys. Rev. D **36**, 3797 (1987).

[18]S. Gottlieb, W. Liu, R. L. Renken, R. L. Sugar, and D. Toussaint, Phys. Rev. D **38**, 2245 (1988).

[19]C. DeTar (private communication).

[20]J. Kogut and E. Dagotto, Phys. Rev. Lett. **59**, 617 (1987); Nucl. Phys. **B295**, 123 (1988).